Available online at www.sciencedirect.com
SCIENCE DIRECT
Brain Research 1046 (2005) 24 – 31
BRAIN RESEARCH
www.elsevier.com/locate/brainres

Research report

Activation of presynaptic $GABA_A$ receptors increases spontaneous glutamate release onto noradrenergic neurons of the rat locus coeruleus

Hitoshi Koga[a], Hitoshi Ishibashi[a], Hideki Shimada[a], Il-Sung Jang[b], Tomoe Y. Nakamura[a], Junichi Nabekura[b,*]

[a]*Cellular and System Physiology, Graduate School of Medical Sciences, Kyushu University, Fukuoka 812-8582, Japan*
[b]*Department of Developmental Physiology, Division of Homeostatic Development, National Institute for Physiological Sciences, Okazaki 444-8585, Japan*

Accepted 15 March 2005
Available online 17 May 2005

Abstract

In order to further explore how GABA can modulate the excitability of noradrenergic neurons of the locus coeruleus (LC), we investigated the presence of $GABA_A$ receptors on glutamatergic nerve terminals and the functional consequences of their activation. We used mechanically dissociated immature rat LC neurons with adherent nerve terminals and patch-clamp recordings of spontaneous excitatory postsynaptic currents. Activation of presynaptic $GABA_A$ receptors by muscimol facilitated spontaneous glutamate release by activating tetrodotoxin-sensitive Na^+ channels and high-threshold Ca^{2+} channels. Bumetanide (10 μM), a potent blocker of Na^+–K^+–Cl^- cotransporter, diminished the muscimol-induced facilitatory action of glutamate release. Our results indicate that the Na^+–K^+–Cl^- cotransporter accumulates Cl^- inside the nerve terminals so that activation of presynaptic $GABA_A$ receptors causes depolarization. This $GABA_A$-receptor-mediated modulation of spontaneous glutamatergic transmission is another mechanism by which GABA and its analogues can regulate the excitability and activity of noradrenergic neurons in the LC.

Theme: Excitable membranes and synaptic transmission
Topic: Mechanisms of neurotransmitter release

Keywords: Spontaneous EPSC; NKCC; Muscimol; Presynaptic Ca^{2+} channels

1. Introduction

The locus coeruleus (LC) contains large clusters of noradrenaline-containing neurons (A6 cell group) which project widely throughout the central nervous system (CNS) [49]. The LC plays important roles in the control of cognitive and emotional processes, including attention and anxiety [7,13]. LC neurons typically spontaneously fire action potentials [3,50] and this firing rate is altered by a variety of sensory stimuli and is particularly modulated by the sleep–wake cycle [5,21]. LC neurons show their highest level of activity during active waking, decrease their firing frequency during slow wave sleep, and are almost silent during rapid eye movement sleep [4]. At a cellular level, the excitability of LC neurons is regulated by both excitatory and inhibitory synaptic inputs. For instance, the in vivo iontophoretic application of glutamate receptor agonists increases the firing frequency [8], whereas iontophoretic application of γ-aminobutyric acid (GABA) suppresses the activity of LC neurons [12]. However, the systemic or intracerebroventricular administration of GABA-mimetics has a facilitatory effect on central noradrenergic neurons [2,11] and enhances the catecholamine current measured by in vivo voltammetry [40].

GABA is the primary inhibitory neurotransmitter throughout the mammalian CNS. Activation of ionotropic $GABA_A$ receptors increases the Cl^- conductance of membrane. This results in postsynaptic hyperpolarization

* Corresponding author.
E-mail address: nabekura@nips.ac.jp (J. Nabekura).

0006-8993/$ - see front matter © 2005 Elsevier B.V. All rights reserved.
doi:10.1016/j.brainres.2005.03.026

in adult neurons, although in developing and injured neurons, Cl^- channel activation causes a depolarization because of the high intracellular Cl^- concentration [10,17,27,35]. These GABA-induced depolarizations can elevate the intracellular Ca^{2+} concentration via activation of voltage-dependent Ca^{2+} channels [29] and this is thought to contribute to synapse maturation. A $GABA_A$-receptor-mediated depolarization has also been observed in mature presynaptic nerve terminals [23,24,41,44]. In sensory afferent terminals, the activation of presynaptic $GABA_A$ receptors induces presynaptic inhibition of action-potential evoked transmitter release by inactivating Na^+ channels and/or shunting the presynaptic membrane potential [41,44]. In contrast, the presynaptic depolarization induced by $GABA_A$ receptor activation increases spontaneous transmitter release [23,24]. Such $GABA_A$-receptor-mediated presynaptic depolarization also results from a higher intraterminal Cl^- concentration, resulting from inwardly directed Cl^- transport mechanism such as the Na–K–Cl cotransporter (NKCC) [23,27,48].

Direct iontophoretic application of GABA to the LC in brain slices reduces the firing rate of rat LC neurons in a manner sensitive to the $GABA_A$ receptor blocker, bicuculline [45]. However, it is not clear whether this is mediated solely through postsynaptic $GABA_A$ receptors or whether presynaptic $GABA_A$ receptors also contribute. Capsaicin, for example, increases the activity of LC neurons by acting on presynaptic VR1 receptors to increase spontaneous glutamate release, without affecting either evoked release or without directly acting on LC neurons [31]. We therefore hypothesized that GABA might also affect LC noradrenergic neuron excitability by acting on glutamatergic presynaptic terminals. To test this, we studied the effects of the $GABA_A$ receptor agonist, muscimol, on spontaneous excitatory postsynaptic currents (sEPSCs) recorded in juvenile rat LC neurons which were mechanically isolated so as to retain adherent and functional presynaptic nerve terminals [1].

2. Experimental procedures

2.1. Preparation

Wistar rats (13–17 days old) were decapitated under pentobarbital sodium anesthesia (80 mg/kg, i.p.). The brain was quickly removed and sliced at a thickness of 380 μm using a microslicer (VT1000S; Leica, Nussloch, Germany). Slices were kept in the incubation medium (see below) saturated with 95% O_2 and 5% CO_2 at room temperature (21–24 °C) for at least 1 h before the mechanical dissociation. Slices were then transferred into a 35-mm culture dish (Primaria 3801; Becton Dickinson, Rutherford, NJ, USA), and the region of the LC was identified under a binocular microscope. Details of the mechanical dissociation have been recently reviewed [1].

All experiments were performed under guiding principles for care and use of animals approved by the Council to the Physiological Society of Japan.

2.2. Electrical measurements

The electrical measurements were performed using conventional whole-cell patch-clamp recordings at holding potentials of −60 to −65 mV. Membrane voltage was controlled, and currents recorded, with the use of a patch-clamp amplifier (EPC-7; List Medical, Darmstadt-Eberstadt, Germany). Patch pipettes were made from borosilicate capillary glass in two stages on a vertical pipette puller (PB-7, Narishige, Tokyo, Japan). The resistance between the recording pipettes filled with internal solution and the reference electrode was 4–6 MΩ. Neurons were visualized under phase contrast on an inverted microscope (Diaphot; Nikon, Tokyo, Japan). Current and voltage were continuously monitored on an oscilloscope and a pen recorder (WR3320, Graphtec, Tokyo, Japan). Membrane currents were filtered at 3 kHz (E-3201A; NF Electric Instruments, Tokyo, Japan), digitized at 6 kHz, and stored on a computer equipped with pCLAMP8.0 (Axon Instruments). All experiments were performed at room temperature (21–24 °C).

2.3. Immunostaining for tyrosine hydroxylase (TH) in dissociated LC neurons

We performed immunocytochemical experiments. Dissociated neurons were allowed to settle on to polyethlenimine (PEI)-coated, glass coverslips which were then transferred on to small strips of in a 35-mm culture dish. Coverslips were moved to parafilm sheet for immunocytochemistry. Neurons were fixed with 4% paraformaldehyde in phosphate-buffered saline (PBS) for 30 min at 4 °C, and were then washed with PBS. After treatment with 0.2% Triton X-100 for 5 min at room temperature, neurons were incubated with PBS containing 5% normal bovine serum for 30 min and then incubated with 1% normal bovine serum for 10 min. Neurons were subsequently incubated with PBS containing rabbit anti-tyrosine hydroxylase (TH) antibody (1:1000; Chemicon International) and 1% normal bovine serum for 1.5 h, and then with fluorescein isothiocyanate (FITC)-conjugated donkey anti-rabbit secondary antibody (1:150; Jackson ImmunoResearch Laboratories) for a further 1 h. Neurons were photographed through a microscope with a digital camera (Carl Zeiss, Germany).

2.4. Data analysis

Spontaneous EPSCs were detected and analyzed using the MiniAnalysis program (Synaptosoft, Decatur, GA). Spontaneous events were initially detected automatically, using an amplitude threshold of 3 pA, and then visually

accepted or rejected on the basis of the rise and decay times. Events with brief rise times (0.5–1.5 ms), and with decay times that were well fitted by a single-exponential function were selected for further analysis. The amplitude and interevent intervals of large numbers of sEPSCs obtained from a single neuron were examined by constructing all-point cumulative probability distributions and compared using the Kolmogorov–Smirnov test. Values of $P < 0.05$ were considered significant. Differences in mean sEPSC amplitude and frequency under different conditions were tested with Student's paired two-tailed t test using their absolute values. Values of $P < 0.05$ were considered significant.

2.5. Solutions

The composition of incubation solutions was (in mM): 124 NaCl, 2.5 KCl, 1.2 KH_2PO_4, 24 $NaHCO_3$, 2 $CaCl_2$, 1 $MgCl_2$, and 10 glucose saturated with 95% O_2 and 5% CO_2. The standard external solution consisted of (in mM) 150 NaCl, 2.5 KCl, 2 $CaCl_2$, 1 $MgCl_2$, 10 HEPES, and 10 glucose. This standard external solution was adjusted to pH 7.4 with tris(hydroxymethyl)aminomethane (Tris-base). The ionic composition of the internal (patch pipette) solution was (in mM) 145 Cs-methanesulfonate, 5 tetraethylammonium-Cl, 5 CsCl, 2 EGTA, and 10 HEPES. The pH was adjusted to 7.2 with Tris-base.

2.6. Drugs

Drugs used in the present study were bicuculline (Tocris Cookson, Avonmouth, UK), diazepam (Wako, Tokyo, Japan), muscimol, tetrodotoxin, bumetanide (Sigma, St Louis, MO, USA), ω-conotoxin-MVIIC, and nilvadipine (Peptide Institute, Osaka, Japan). Drugs were applied using 'Y-tube system', which enables rapid solution exchange.

3. Results

3.1. Spontaneous EPSCs in noradrenergic neurons

In order to firstly identify the noradrenergic neurons amongst the acutely dissociated LC neurons, we imaged TH-immunoreactivity. As shown in Fig. 1A, TH-positive neurons had a relatively large soma (≧40 μm) and multiple dendritic processes, while TH-negative neurons were smaller in size (≦20 μm) and often with bipolar dendrites (Fig. 1A). Current deflections representing spontaneous action potentials were typically seen at a frequency of 1.5–5 Hz in cell-attached recordings from these large neurons (Fig. 1B). This observation is consistent with previous reports that LC noradrenergic neurons discharge spontaneous action potentials at 1–4 Hz [3,13]. Thus, the following electrophysiological experiments were only performed on LC neurons with large somas and multiple dendrites.

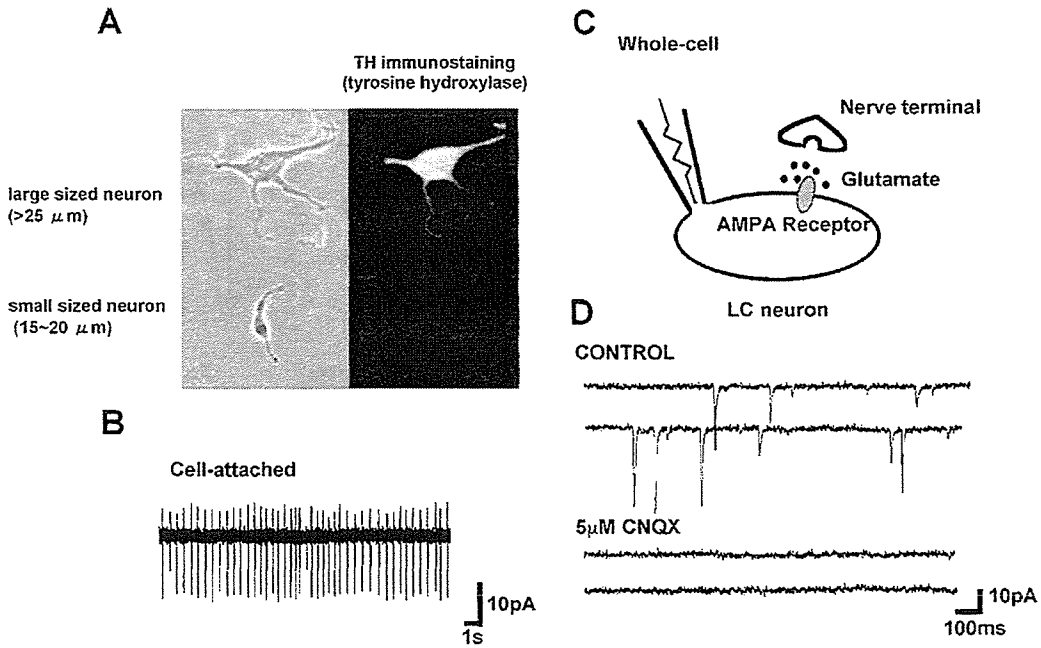

Fig. 1. Spontaneous EPSCs in noradrenergic neurons. (A) TH immunostaining of acutely dissociated LC neurons. Phase contrast (left) and TH immunostainings (right) of the dissociated LC neurons. The TH-positive neurons had a relatively large soma and were multipolar in shape, whereas the TH-negative neuron had a small soma and were often bipolar. (B) Current deflections representing spontaneous firing of action potentials in a large LC neuron recorded in the cell-attached patch-clamp recording mode. (C) Schematic representation of synaptic current recording from the dissociated neuron with adherent nerve terminals. (D) Effect of CNQX on spontaneous postsynaptic currents. Recordings were performed at a holding potential (V_H) of −61 mV using the conventional whole-cell patch recording configuration. The traces were representative of 5 neurons.

The noradrenergic neurons of the LC receive not only glutamatergic inputs, but also GABAergic inputs [43]. To distinguish between $GABA_A$ receptors on the glutamatergic presynaptic terminals synapsing onto the isolated LC neurons from $GABA_A$ receptors on the postsynaptic membrane, we dialyzed the cells with an ATP-free pipette solution for at least 30 min before applying muscimol. This causes a rapid rundown of postsynaptic $GABA_A$ receptor responses [23,42] and allows us to selectively investigate the effects of presynaptic $GABA_A$ receptor activation. In addition, the V_H of the LC neurons was adjusted to about −60 mV which was close to the reversal potential of the muscimol-induced postsynaptic currents in our experimental conditions ($[Cl^-]_i$; 10 mM, $[Cl^-]_o$; 161 mM). Under these conditions, all the spontaneous postsynaptic currents were reversibly inhibited by 5 μM CNQX (Fig. 1D), indicating that they were sEPSCs mediated by non-NMDA type glutamate receptors.

3.2. $GABA_A$-receptor-mediated modulation of spontaneous EPSCs

As shown in Fig. 2, the application of muscimol (1 μM) increased the frequency of sEPSCs from 1.63 ± 0.18 to 3.37 ± 0.36 Hz ($P < 0.001$, $n = 22$). The cumulative distribution of sEPSC interevent intervals was shifted to the left by muscimol, whereas the cumulative distribution of sEPSC amplitude was not affected. (Fig. 2B). These results indicate that muscimol acts presynaptically to facilitate spontaneous glutamate release at these synapses.

To confirm that muscimol facilitates sEPSC frequency via $GABA_A$ receptors, we investigated the effect of bicuculline, a $GABA_A$ receptor antagonist, on this response. The facilitation of sEPSC frequency elicited by 1 μM muscimol was completely blocked in the presence of 5 μM bicuculline (Fig. 3). We also examined the effect of diazepam, a $GABA_A$ receptor allosteric potentiator on the muscimol response (Fig. 4). In 5 neurons tested, a subthreshold dose of muscimol (0.5 μM) had no significant affect on sEPSC frequency. The sEPSC frequency in the absence and presence of 0.5 μM muscimol was 1.47 ± 0.18 and 2.09 ± 0.46 Hz ($n = 5$, $P = 0.112$), respectively. Although diazepam (1 μM) itself did not affect the sEPSC frequency, the co-application of both 0.5 μM muscimol and 1 μM diazepam increased sEPSC frequency from 1.15 ± 0.36 to 3.11 ± 0.60 Hz ($P < 0.01$, $n = 5$).

3.3. Involvement of voltage-dependent Na^+ and Ca^{2+} channels in muscimol-induced facilitation of release

We next examined the possible mechanisms underlying the $GABA_A$-receptor-mediated facilitation of sEPSC frequency. First, we investigated the effect of tetrodotoxin (TTX), a voltage-dependent Na^+ channel blocker. As shown in Fig. 5, application of TTX reduced the basal sEPSC frequency from 1.38 ± 0.26 to 0.64 ± 0.196 Hz. In the presence of TTX, the facilitation of sEPSC frequency by muscimol (1 μM) was completely abolished, indicating a critical contribution of tetrodotoxin-sensitive Na^+ channels to the muscimol response.

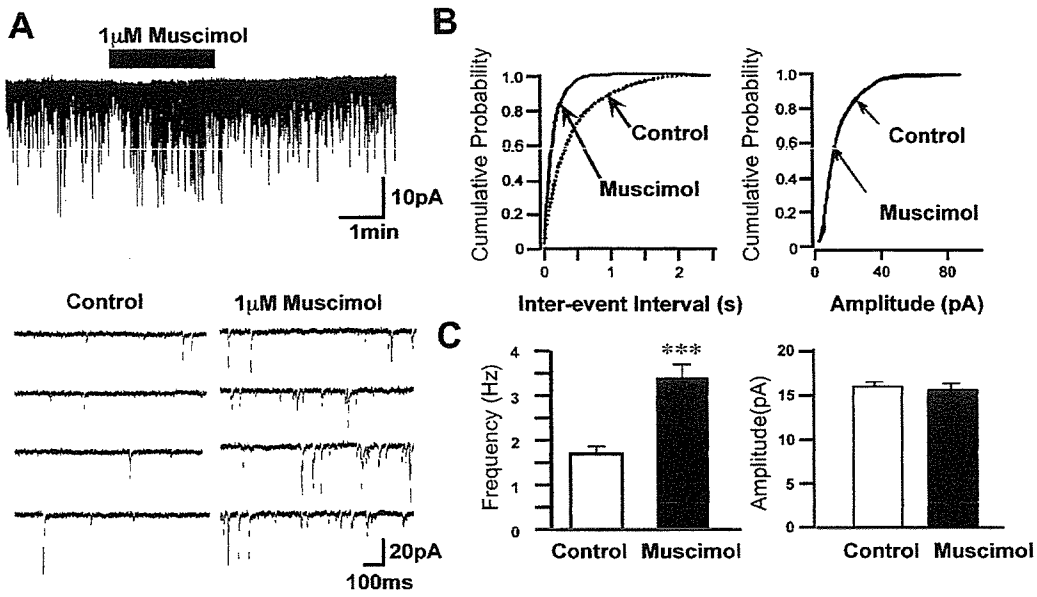

Fig. 2. The effect of muscimol on spontaneous EPSCs. (A) A typical recording of spontaneous EPSCs before, during, and after application of 1 μM muscimol. A portion of currents during control recordings and in the presence of muscimol are shown at greater resolution in the lower panel. (B) Cumulative distributions of interevent intervals (left) and spontaneous EPSC amplitudes (right) in control conditions and in the presence of 1 μM muscimol. All data come from the same neuron as shown in panel A. (C) The mean frequency and amplitude of spontaneous EPSCs recorded under control conditions and in the presence of muscimol (1 μM). The mean data come from 22 neurons. ***$P < 0.001$.

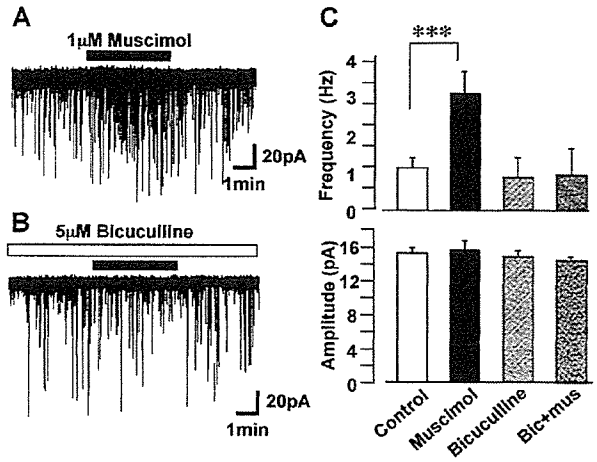

Fig. 3. Inhibition by bicuculline of the muscimol-induced increase in spontaneous EPSC frequency. (A and B) Typical current traces of spontaneous EPSCs observed before, during, and after application of 1 μM muscimol in the absence (A) or continued presence (B) of 5 μM bicuculline. (C) Histograms showing the mean affects of bicuculline on the muscimol response. Data have been averaged from 3 neurons. Bic: bicuculline; Mus: muscimol; ***$P < 0.01$.

We next examined the effect of Cd^{2+}, a general blocker of voltage-dependent Ca^{2+} channels, on the muscimol response. Application of Cd^{2+} (100 μM), by itself, reduced basal sEPSC frequency to 36.2 ± 12.8% (n = 3) of the control rate ($P < 0.01$). In the presence of Cd^{2+}, the muscimol-induced facilitation was completely abolished (Fig. 6). However, because Cd^{2+} itself may directly block $GABA_A$ receptors [28], we also tested the effects of nilvadipine, an L-type Ca^{2+} channel antagonist [22], and ω-conotoxin-MVIIC, a blocker of N- and P/Q-type Ca^{2+} channels [20]. Both nilvadipine (0.3 μM) and ω-conotoxin-MVIIC (3 μM) reduced the basal sEPSC frequency, to 56.3 ± 6.9 (n = 5) and 44.7 ± 5.8% (n = 4) of control, respectively. In the presence of 0.3 μM nilvadipine, however, muscimol (1 μM) still increased sEPSC frequency, to 197.2 ± 27.2% (n = 7; Fig. 6). This is comparable to the extent of facilitation seen in the absence of nilvadipine. In contrast, 3 μM ω-conotoxin-MVIIC completely abolished the muscimol action (Fig. 6). These results suggest the contribution of N- and/or P/Q-type high-voltage-activated Ca^{2+} channels to the muscimol-induced facilitation of glutamate release.

3.4. Contribution of the Na–K–Cl cotransporter to the muscimol response

Since the muscimol-induced facilitation of sEPSC frequency depended critically on the activation of voltage-dependent Na^+ and Ca^{2+} channels, it is reasonable to conclude that the activation of presynaptic $GABA_A$ receptors depolarizes the glutamatergic nerve terminals. This may result from Cl^- efflux, which implies that the intraterminal Cl^- concentration is maintained higher than that predicted for a passive distribution. If this is indeed the case, a higher intraterminal Cl^- concentration might be established by some inwardly directed Cl^- transport systems, such as

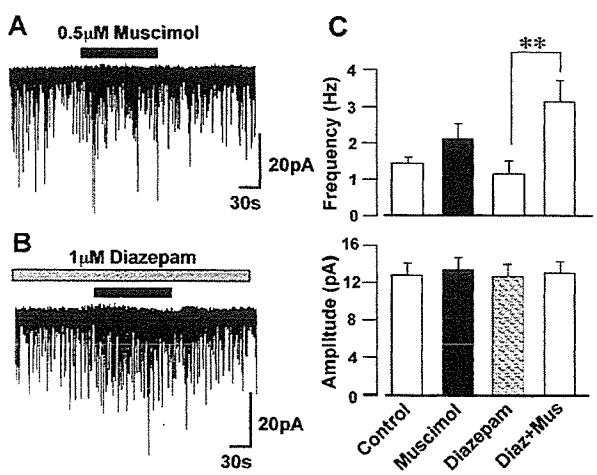

Fig. 4. Effect of diazepam on the muscimol-induced increase in spontaneous EPSC frequency. (A and B) Typical current traces of spontaneous EPSCs observed before, during, and after application of 0.5 μM muscimol in the absence (A) or continued presence (B) of 1 μM diazepam. (C) Histograms showing the mean affects of diazepam on the muscimol response. Data have been averaged from 5 neurons. Diaz: diazepam; Mus: muscimol; **$P < 0.01$.

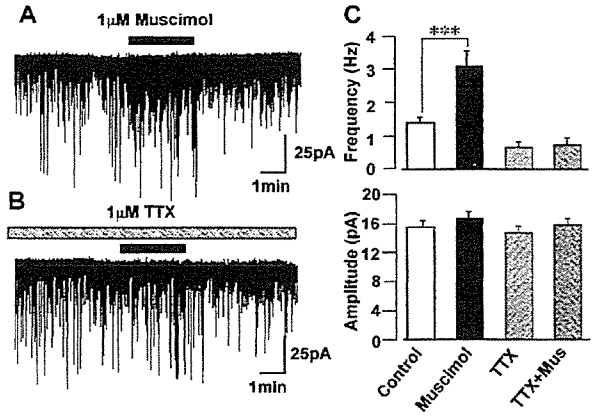

Fig. 5. Effect of tetrodotoxin (TTX) on the muscimol-induced facilitation of spontaneous EPSC frequency. (A and B) Typical current traces of spontaneous EPSCs observed before, during, and after application of 1 μM muscimol in the absence (A) or continued presence (B) of 1 μM TTX. (C) Histograms showing the mean affects of diazepam on the muscimol response. Data have been averaged from 5 neurons. Mus: muscimol; ***$P < 0.01$.

NKCC and/or the Cl^--HCO_3^- exchanger [26,38,39]. In immature and injured CNS neurons and sensory neurons, the Na–K–Cl cotransporter has an important role in raising the intracellular Cl^- concentration and hence causing GABA-induced depolarizations [27,35,39]. Furthermore, NKCC generates the Cl^- accumulation in glutamatergic nerve terminals projecting onto rat ventromedial hypothalamic neurons [23]. To investigate any contribution of NKCC to the muscimol-induced facilitation of release, we employed bumetanide, a potent blocker of NKCC [19].

The first application of muscimol in the presence of 10 μM bumetanide, a concentration which is specific for

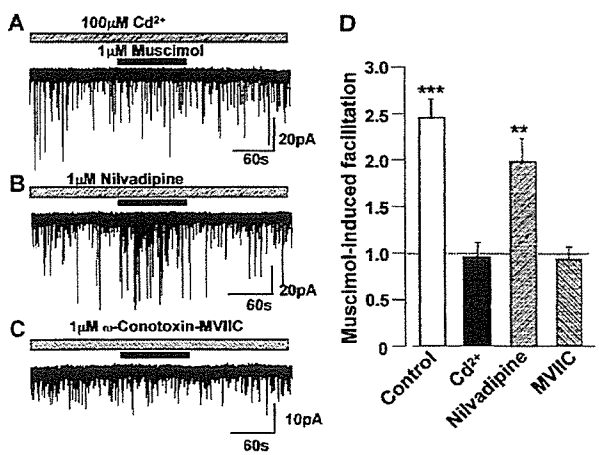

Fig. 6. Effects of Ca^{2+}-antagonists on the muscimol action. (A, B, and C) Typical current traces of spontaneous EPSCs observed before, during, and after application of 1 μM muscimol, all in the continued presence of 100 μM Cd (A), 1 μM nilvadipine (B), or 1 μM ω-conotoxin-MVIIC (C). The 3 traces were obtained from the same neuron. (D) Histograms showing the mean affects of the different Ca^{2+} channel blockers on the muscimol-induced enhancement of spontaneous EPSC frequency. Data have been averaged from 5 neurons. **$P < 0.01$, ***$P < 0.001$.

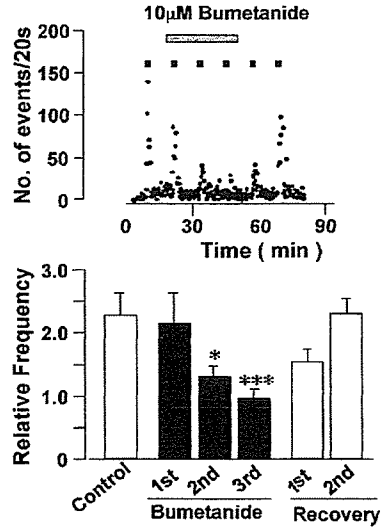

Fig. 7. Effect of bumetanide, an inhibitor of the Na–K–Cl cotransporter, on muscimol-induced facilitation of spontaneous EPSC frequency. Histograms show the relative facilitation of spontaneous EPSC frequency in response to muscimol alone, and then in response to 3 separate applications of muscimol in the continued presence of bumetinide, and again following bumetinide washout. Each column is the mean of data from 4 neurons and sEPSC frequency has been normalized to the control value. *$P < 0.05$, ***$P < 0.001$.

NKCC, induced nearly the same facilitatory effect as that observed in control conditions. However, subsequent applications of muscimol, in the continued presence of bumetanide, caused smaller amounts of facilitation and facilitation was absent on the third muscimol application (Fig. 7). The muscimol response slowly recovered back to control values after washing out bumetanide (Fig. 7). This result suggests that functional NKCC are present on these glutamatergic nerve terminals where they contribute to the maintenance of a high intraterminal Cl^- concentration.

4. Discussion

The present study demonstrates that $GABA_A$ receptors are present on glutamatergic nerve terminals projecting to noradrenergic neurons in the rat LC, and that their activation depolarizes these nerve terminals causing an increase in spontaneous glutamate release. This $GABA_A$-receptor-mediated depolarization seems to occur as a result of bumetanide-sensitive inwardly directed presynaptic NKCC transporters accumulating Cl^- in the terminals.

In mature CNS neurons, $GABA_A$ receptor activation generally hyperpolarizes the neuronal membrane as Cl^- ions enter the cell down their electrochemical gradient. In contrast, in immature neurons in the central and peripheral nervous system, $GABA_A$ receptor activation by exogenous or synaptically released GABA causes depolarization and neuronal excitation [6,27,33,36]. This depolarization can activate voltage-dependent Na^+ and Ca^{2+} channels to cause an increase in the postsynaptic intracellular Ca^{2+} concen-

tration [19,29,36,37]. The present study indicates that the $GABA_A$-receptor-induced depolarization activates voltage-dependent Na^+ channels causing an activation of voltage-dependent Ca^{2+} channels and facilitation of glutamate release. A similar sequence of events occurs following activation of presynaptic $GABA_A$ receptors on excitatory terminals projecting to rat ventral–medial hypothalamic neurons and for both glycine and $GABA_A$ receptors on glycinergic terminals projecting to sacral dorsal commissural neurons in the rat spinal cord [23–25].

Blockade of muscimol response by TTX may also suggest that the presynaptic $GABA_A$-receptor-mediated depolarization failed to directly activate presynaptic voltage-dependent Ca^{2+} channels. This is possibly because the amplitude of the depolarization was insufficient or because of the spatial distribution of the channels relative to the GABA receptors. N- and P/Q-type Ca^{2+} channels are reported to exist near the release site in the presynaptic terminals, and Ca^{2+} influx through these channels plays a key role in the transmitter release [32,46]. ω-Conotoxin-MVIIC, a blocker of these channels, reduced basal spontaneous EPSC frequency and abolished the facilitatory effect of muscimol. On the other hand, L-type Ca^{2+} channels have been reported to be localized at presynaptic boutons some distance from the neurotransmitter release site and hence Ca^{2+} influx through L-type Ca^{2+} channels does not directly trigger neurotransmitter release [32]. L-type Ca^{2+} channels may, however, play some role in propagating action potentials down to the release sites [30,34]. Thus, the reduction of the basal spontaneous EPSC frequency by the L-type channel blocker, nilvadipine, may be due to a decrease in Ca^{2+}-mediated action potentials which then propagate to the release sites. Niveldipine did not, however, affect the muscimol-induced facilitation, suggesting that this response may be localized closer to the release sites.

Direct iontophoretic application of GABA has an inhibitory effect on the LC neurons [45]. Thus, before starting this study, we hypothesized that GABA might reduce the EPSC frequency. But, the present results are contrary to these expectations. One possible clinical relation to our present results concerns the role of the LC in anxiety and panic disorders. Noradrenaline release from the LC enhances anxiety [9,13,14,16] and treatment for this illness often involves the benzodiazepines. A reduction in LC activity due to a potentiation of postsynaptic LC $GABA_A$ receptors is thought to contribute to their anti-anxiety actions [14,15]. However, depression, agitated toxic psychosis, hypomanic and manic behavior, increased anxiety, increased hostility and paradoxical rage reactions have all been reported to be caused by the benzodiazepines [18]. Our current results suggest that the benzodiazepine enhances the glutamate release by muscimol onto LC neurons. That may increase noradrenaline release from LC neurons. Furthermore, there are several reports suggesting that systemic or intracerebroventricular injection of GABA enhances noradrenaline synthesis and utilization rate [2,11]. Scatton and Serrano [40] reported that systemic administration of muscimol enhanced the catechol current measured in the LC by in vivo voltammetry. GABA is also reported to increase evoked noradrenaline release from rat cortical slices [47]. An increase of glutamate release to the LC neurons by GABA might be one mechanism contributing to these excitatory actions of GABA and muscimol on LC activity and to the paradoxical benzodiazepine-induced enhancement of anxiety.

Acknowledgments

We thank Dr. A. Moorhouse for discussion and editing of the manuscript. This work was supported by research grants from the Ministry of Education, Culture, Sports, Science and Technology, Japan (15016082, 15650076 and 15390065 to J.N.). This work was also supported by CREST, JST.

References

[1] N. Akaike, A.J. Moorhouse, Techniques: applications of the nerve-bouton preparation in neuropharmacology, Trends Pharmacol. Sci. 24 (2003) 44–47.
[2] S. Arbilla, S.Z. Langer, Facilitation by GABA of the potassium evoked release of ^{3}H-noradrenaline from the rat occipital cortex, Naunyn-Schmiedeberg's Arch. Pharmacol. 306 (1979) 161–168.
[3] J. Arima, C. Kubo, H. Ishibashi, N. Akaike, α_2-Adrenoceptor-mediated potassium currents in acutely dissociated rat locus coeruleus neurons, J. Physiol. 508 (1998) 57–66.
[4] G. Aston-Jones, F.E. Bloom, Activity of norepinephrine-containing locus coeruleus neurons in behaving rats anticipates fluctuations in the sleep–waking cycle, J. Neurosci. 18 (1998) 67–886.
[5] G. Aston-Jones, J. Rajkowski, J. Cohen, Locus coeruleus and regulation of behavioral flexibility and attention, Prog. Brain Res. 126 (2000) 165–182.
[6] K. Ballanyi, P. Grafe, An intracellular analysis of γ-aminobutyric-acid-associated ion movements in rat sympathetic neurons, J. Physiol. 365 (1985) 41–58.
[7] C.W. Berridge, B.D. Waterhouse, The locus coeruleus–noradrenergic system; modulation of behavioral state and state-dependent cognitive processes, Brain Reserch Reviews 42 (2003) 33–84.
[8] P.J. Charlety, K. Chergui, H. Akaoka, C.F. Saunier, M. Buda, G. Aston-Jones, G. Chouvet, Serotonin differentially modulates responses mediated by specific excitatory amino acid receptors in the rat locus coeruleus, Eur. J. Neurosci. 5 (1993) 1024–1028.
[9] D.S. Charney, G.R. Heninger, A. Breier, Noradrenergic function in panic anxiety. Effects of yohimbine in healthy subjects and patients with agoraphobia and panic disorder, Arch. Gen. Psychiatry 41 (8) (1984 (Aug.)) 751–763.
[10] G. Chen, P.Q. Trombley, A.N. van den Pol, Excitatory actions of GABA in developing rat hypothalamic neurons, J. Physiol. (London) 494 (1996) 451–464.
[11] T. Dennis, O. Curet, T. Nishikawa, B. Scatton, Further evidence for, and nature of, the facilitatory GABAergic influence on central noradrenergic transmission, Naunyn-Schmiedeberg's Arch. Pharmacol. 331 (1985) 225–234.
[12] M. Ennis, G. Aston-Jones, GABA-mediated inhibition of locus coeruleus from the dorsomedial rostral medulla, J. Neurosci. 9 (1989) 2973–2981.
[13] S.L. Foote, F.E. Bloom, G. Aston-Jones, Nucleus locus coeruleus: new

evidence of anatomical and physiological specificity, Physiol. Rev. 63 (1983) 844–914.
[14] A.W. Goddard, S.W. Woods, D.S. Charney, A critical review of the role of norepinephrine in panic disorder: focus on its interaction with serotonin, in: H.G.M. Westenberg, et al., (Eds.), Advances in the Neurobiology of Anxiety Disorders, Wiley, New York, 1996, pp. 107–137.
[15] A.W. Goddard, T. Brouette, A. Almai, Early coadministration of clonazepam with sertraline for panic disorder, Arch. Gen. Psychiatry 58 (2001) 681–686.
[16] J.M. Gorman, Ventilatory physiology of patients with panic disorder, Arch. Gen. Psychiatry 45 (1988) 31–39.
[17] T.G. Hales, M.J. Sanderson, A.C. Charles, GABA has excitatory actions on GnRH-secreting immortalized hypothalamic (GT1-7) neurons, Neuroendocrinology 59 (1994) 297–308.
[18] R.C. Hall, S. Zisook, Paradoxical reactions to benzodiazepines, Br. J. Clin. Pharmacol. 11 (Suppl. 1) (1981) 99S–104S.
[19] M. Haas, Properties and diversity of (Na–K–Cl) cotransporters, Annu. Rev. Physiol. 51 (1989) 443–557.
[20] D.R. Hillyard, V.D. Monje, I.M. Mintz, B.P. Bean, L. Nadasdi, J. Ramachandran, G. Miljanich, A. Azimi-Zoonooz, J.M. McIntosh, L.J. Cruz, J.S. Imperial, B.M. Olivera, A new conus pepetide ligand for mammalian presynaptic Ca^{2+} channels, Neuron 9 (1992) 69–77.
[21] J.A. Hobson, R.W. McCarley, P.W. Wyzinski, Sleep cycle oscillation: reciprocal discharge by two brainstem neuronal groups, Science 189 (1975) 55–58.
[22] H. Ishibashi, Y. Murai, N. Akaike, Effect of nilvadipine on the voltage-dependent Ca^{2+} channels in rat hippocampal CA1 pyramidal neurons, Brain Res. 813 (1998) 121–127.
[23] I.-S. Jang, H.-J. Jeong, N. Akaike, Contribution of the Na–K–Cl cotransporter on $GABA_A$ receptor-mediated presynaptic depolarization in excitatory nerve terminals, J. Neurosci. 21 (2001) 5962–5972.
[24] I.-S. Jang, H.-J. Jeong, S. Katsurabayashi, N. Akaike, Functional roles of presynaptic $GABA_A$ receptors on glycinergic nerve terminals in the rat spinal cord, J. Physiol. 541 (2002) 423–434.
[25] H.-J. Jeong, I.-S. Jang, A.J. Moorhouse, N. Akaike, Activation of presynaptic glycine receptors facilitates glycine release from presynaptic terminals synapsing onto rat spinal sacral dorsal commissural nucleus neurons, J. Physiol. 550 (Pt. 2) (2003 (Jul. 15)) 373–383.
[26] K. Kaila, Ionic basis of $GABA_A$ receptor channel function in the nervous system, Prog. Neurobiol. 42 (1994) 489–537.
[27] Y. Kakazu, N. Akaike, S. Komiyama, J. Nabekura, Regulation of intracellular chloride by cotransporters in developing lateral superior olive neurons, J. Neurosci. 19 (1999) 2843–2851.
[28] E. Kumamoto, Y. Murata, Characterization of GABA current in rat septal cholinergic neurons in culture and its modulation by metal cations, J. Neurophysiol. 74 (1995) 2012–2027.
[29] X. Leinekugel, V. Tseeb, Y. Ben-Ari, P. Bregestovski, Synaptic $GABA_A$ activation induces Ca^{2+} rise in pyramidal cells and interneurons from rat hippocampal slices, J. Physiol. (London) 487 (1995) 319–329.
[30] F.M. Lu, K. Kuba, Synchronous and asynchronous exocytosis induced by subthreshold high K^+ at Cs^+-loaded terminals of rat hippocampal neurons, J. Neurophysiol. 87 (2002) 1222–1233.
[31] S. Marinelli, C.W. Vaughan, M.J. Christie, M. Connor, Capsaicin activation of glutamatergic synaptic transmission in the rat locus coeruleus in vitro, J. Physiol. 543 (2002) 531–540.
[32] R.J. Miller, Multiple calcium channels and neuronal function, Science 235 (1987) 46–52.
[33] U. Misgeld, R.A. Deisz, H.U. Dodt, H.D. Lux, The role of chloride transport in postsynaptic inhibition of hippocampal neurons, Science 232 (1986) 1413–1415.
[34] N. Murakami, H. Ishibashi, S. Katsurabayashi, N. Akaike, Calcium channel subtypes on single GABAergic presynaptic terminal projecting to rat hippocampal neurons, Brain Res. 951 (2002) 121–129.
[35] J. Nabekura, T. Ueno, A. Okabe, A. Furuta, T. Iwaki, C. Shimizu-Okabe, A. Fukuda, N. Akaike, Reduction of KCC2 expression and $GABA_A$ receptor-mediated excitation after in vivo axonal injury, J. Neurosci. 22 (2002) 4412–4417.
[36] K. Obrietan, A.N. van den Pol, GABA neurotransmission in the hypothalamus: developmental reversal from Ca^{2+} elevating to depressing, J. Neurosci. 15 (1995) 5065–5077.
[37] D.F. Owens, L.H. Boyce, B.E. Davis, A.R. Kriegstein, Excitatory GABA responses in embryonic and neonatal cortical slices demonstrated by gramicidin perforated-patch recordings and calcium imaging, J. Neurosci. 16 (1996) 6414–6423.
[38] M.D. Plotkin, E.Y. Snyder, S.C. Hebert, E. Delpire, Expression of the Na–K–2Cl cotransporter is developmentally regulated in postnatal rat brain: a possible mechanism underlying GABA's excitatory role in immature brain, J. Neurobiol. 33 (1997) 781–795.
[39] J.M. Russell, Sodium–potassium–chloride cotransport, Physiol. Rev. 80 (2000) 211–276.
[40] B. Scatton, A. Serrano, GABA mimetics increase extracellular DOPAC (as measured by in vivo voltammetry) in the rat locus coeruleus, Naunyn-Schmiedeberg's Arch. Pharmacol. 332 (1986) 380–383.
[41] I. Segev, Computer study of presynaptic inhibition controlling the spread of action potentials into axon terminals, J. Neurophysiol. 63 (1990) 987–998.
[42] T. Shirasaki, K. Aibara, N. Akaike, Direct modulation of $GABA_A$ receptor by intracellular ATP in dissociated nucleus tractus solitarii neurones of rat, J. Physiol. 449 (1992) 551–572.
[43] N. Singewald, A. Philippu, Release of neurotransmitters in the locus coeruleus, Prog. Neurobiol. 56 (1998) 237–267.
[44] G.J. Stuart, S.J. Redman, The role of $GABA_A$ and $GABA_B$ receptors in presynaptic inhibition of Ia EPSPs in cat spinal motoneurones, J. Physiol. 449 (1992) 551–572.
[45] S.T. Szabo, P. Blier, Serotonin (1A) receptor ligands act on norepinephrine neuron firing through excitatory amino acid and GABA(A) receptors: a microiontophoretic study in the rat locus coeruleus, Synapse 42 (2001) 203–212.
[46] T. Takahashi, A. Momiyama, Different types of calcium channels mediate central synaptic transmission, Nature 366 (1993) 156–158.
[47] H.D. Taube, K. Starke, E. Borowski, Presynaptic receptor systems on the noradrenergic neurons of the rat brain, Naunyn-Schmiedeberg's Arch. Pharmacol. 299 (1977) 123–141.
[48] S. Uchida, E. Noda, Y. Kakazu, Y. Mizoguchi, N. Akaike, J. Nabekura, Allopregnanolone enhancement of GABAergic transmission in rat medial preoptic area neurons, Am. J. Physiol.: Endocrinol. Metab. 283 (2002) E1257–E1265.
[49] U. Ungerstedt, Stereotaxic mapping of the monoamine pathways in the rat brain, Acta Physiol. Scand. 367 (1971) 1–48 (Suppl.).
[50] J.T. Williams, R.A. North, Catecholamine inhibition of calcium action potentials in rat locus coeruleus neurons, Neuroscience 14 (1985) 103–109.

Available online at www.sciencedirect.com
SCIENCE DIRECT®
Cellular Immunology 231 (2004) 20–29
Cellular Immunology
www.elsevier.com/locate/ycimm

Exosomes secreted from monocyte-derived dendritic cells support in vitro naive CD4$^+$ T cell survival through NF-κB activation☆

Kotaro Matsumoto[a,1], Takashi Morisaki[a], Hideo Kuroki[a], Makoto Kubo[a], Hideya Onishi[a], Katsuya Nakamura[a], Chihiro Nakahara[a], Hirotaka Kuga[a], Eishi Baba[a], Masafumi Nakamura[a], Kazuho Hirata[b], Masao Tanaka[c], Mitsuo Katano[a,*]

[a] *Department of Cancer Therapy and Research, Graduate School of Medical Sciences, Kyushu University, Fukuoka, Japan*
[b] *Department of Anatomy and Cell Biology, Graduate School of Medical Sciences, Kyushu University, Fukuoka, Japan*
[c] *Department of Surgery and Oncology, Graduate School of Medical Sciences, Kyushu University, Fukuoka, Japan*

Received 9 August 2004; accepted 4 November 2004
Available online 11 January 2005

Abstract

We investigated the effect of exosomes secreted from human monocyte-derived dendritic cells (Mo-DCs), which are generated from PBMCs in response to treatment with GM-CSF and IL-4, on naive CD4$^+$ T cell survival in vitro. Exosomes isolated from culture supernatants of Mo-DCs (>90% purity) were purified with anti-HLA-DP, -DQ, -DR-coated paramagnetic beads. Purified exosomes prolonged the survival of naive CD4$^+$ T cells (>98% purity) in vitro. Treatment with neutralizing mAb against HLA-DR significantly decreased the supportive effect of purified exosomes on CD4$^+$ T cell survival. Exosomes increased nuclear translocation of NF-κB in naive CD4$^+$ T cells, and NF-κB activation was significantly suppressed by anti-HLA-DR mAb or NF-κB inhibitor pyrrolidine dithiocarbamate (PDTC). In addition, PDTC inhibited the effect of exosomes on naive CD4$^+$ T cell survival. Thus, exosomes secreted by Mo-DCs appear to support naive CD4$^+$ T cell survival via NF-κB activation induced by interaction of HLA-DR and TCRs.

Keywords: Human monocyte-derived dendritic cells; Multivesicular body; Small membrane vesicle; TCR and MHC interaction

1. Introduction

Prolonged survival of naive CD4$^+$ T cells requires direct contact with self-MHC class II ligands in vivo [1–3]. CD8$^+$ T cells also require exposure to specific self-MHC class I proteins for prolonged survival [4]. Thus, interaction between TCR and MHC molecules plays an important role in supporting naive T cell survival in vivo [5,6]. However, there are few reports concerning the role of TCR and MHC interaction in short-term survival of naive CD4$^+$ T cells in vitro [7].

Exosomes were initially described as microvesicles containing 5′-nucleotidase activity and released from neoplastic cell lines [8,9]. Electron microscopy has shown that exosomes have a characteristic saucer-like morphology of a flattened sphere limited by a lipid bilayer. They range from 30 to 100 nm in diameter [10]. The most common procedure for purifying exosomes from cell-culture supernatants involves a series of centrifugations to remove dead cells and large debris, followed by a final high-speed ultracentrifugation to pellet the exosomes [11,12]. It is generally believed that exosomes are

☆ This work is supported in part by a Grant for Scientific Research (13470240) from the Ministry of Education, Science and Culture, Japan.
* Corresponding author. Fax: +81 92 642 6221.
E-mail address: mkatano@tumor.med.kyushu-u.ac.jp (M. Katano).
[1] Present address: Department of Surgery and Oncology, Graduate School of Medical Sciences, Kyushu University, Fukuoka, Japan.

0008-8749/$ - see front matter © 2004 Elsevier Inc. All rights reserved.
doi:10.1016/j.cellimm.2004.11.002

membrane vesicles that form within late endocytic compartments, multivesicular bodies (MVBs), and are secreted upon fusion of these compartments with the plasma membrane of living cells. As a result, all exosomal proteins reported up to now have been found in the cytosol, in the membrane of endocytic compartments, or at the plasma membrane. Various cell types secrete exosomes. APCs such as dendritic cells (DCs)[2] and B cells also secrete exosomes. Recent advances in biotechnology have made it possible to generate DC-like cells, monocyte-derived DCs (Mo-DCs), in vitro from PBMCs upon treatment with GM-CSF and IL-4 [13], and Mo-DCs secrete exosomes [14]. MHC class II proteins are very abundant in exosomes from Mo-DCs as well as other APCs [15]. In addition, APC-derived exosomes contain specific proteins, such as CD86 and integrins, which are involved in antigen presentation, suggesting a role of exosomes in T cell stimulation [16–18]. In fact, it has been shown that EBV-transformed B cell-derived exosomes stimulate human $CD4^+$ T cell clones in an antigen-specific manner [10]. T cell stimulation by exosomes produced by rat mast cells engineered to express mouse or human MHC class II proteins has been reported [19]. Interestingly, exosomes produced by tumor peptide-pulsed DCs induce T cell-dependent tumor rejection in vivo [14].

NF-κB is a transcription factor that is activated in T cells by interaction between TCRs and MHC class I or class II proteins [20–22] and has been shown to play an important role in the expression of anti-apoptotic genes [23]. In most resting cells, NF-κB is located in the cytoplasm as a heterodimer of the structurally related proteins p50, p52, RelA, c-Rel, and RelB. All of these are noncovalently associated with the cytoplasmic inhibitor IκB [24]. The most common NF-κB is the p65/p50 heterodimer. Activation of NF-κB is preceded by phosphorylation of IκB by IκB kinase, which is followed by proteolytic removal of IκB and movement of NF-κB to the nucleus. Nuclear translocation of NF-κB is thought to reflect its activation [25]. Zheng et al [26] reported a critically important function of NF-κB in TCR-induced regulation of $CD4^+$ T cell survival in p50−/− cRel−/− mice. In addition, survival of antigen-stimulated T cells requires NF-κB-mediated inhibition of p73 expression [22]. Thus a role of NF-κB in T cell survival appears to be important. However, a role of the NF-κB-activating pathway in naive $CD4^+$ T cell survival has not been identified in human cells.

Here, we report for the first time that Mo-DC-derived exosomes support naive $CD4^+$ T cell survival in vitro through interaction between TCRs and human leukocyte antigen (HLA)-DR, and that TCR-dependent NF-κB activation may contribute to this survival.

2. Materials and methods

2.1. Reagents

Pyrrolidine dithiocarbamate (PDTC), an inhibitor of NF-κB nuclear translocation, was purchased from Sigma Chemical (Deisenhofen, Germany).

2.2. Preparation of human Mo-DCs and naive $CD4^+$ T cells

Mo-DCs were generated from the adherent fraction of PBMCs from healthy volunteers, as previously described but with minor modifications [13]. Briefly, PBMCs were isolated from heparinized peripheral blood by Ficol–Paque (Life Technologies, Gaithersburg, MD, USA) density gradient centrifugation. PBMCs were resuspended in RPMI 1640 basal medium (Sanko Pure Chemicals, Tokyo Japan) supplemented with 1% human albumin (Mitsubishi Pharma, Osaka, Japan), 100 μg/ml penicillin (Meijiseika, Tokyo, Japan), and 100 μg/ml streptomycin (Meijiseika) (RPMI medium), plated at a density of 2×10^6 cells/ml, and allowed to adhere overnight at 37 °C in 24-well plates (Nalge Nunc International, Chiba, Japan). Nonadherent cells were removed, and adherent cells were cultured in RPMI medium containing GM-CSF (100 ng/ml, North China Pharmaceutical Group, Shijiazhuang, China) and IL-4 (50 ng/ml, Osteogenetics, Wurzburg, Germany). On day 7, nonadherent fractions were collected as Mo-DCs. Mo-DCs were further purified by negative selection with magnetic beads coated with mouse monoclonal anti-CD2, anti-CD3, and anti-CD19 antibodies (Dynabeads, Dynal Biotech, Oslo, Norway). This depletion procedure yielded over 90% $CD14^-$, $CD80^+$, and $HLA\text{-}DR^+$ Mo-DCs as assessed by fluorescence-activated cell sorting (FACS) (FACS Calibur flow cytometer, Becton–Dickinson Immunocytochemistry Systems, Franklin Lakes, NJ, USA) and analyzed with CELLQuest software (Becton–Dickinson).

Seven days after the initial culture of nonadherent cells, PBMCs were collected again from the same healthy volunteer. $CD4^+$ T cells were purified from fresh human PBMCs with a CD4-positive isolation kit (Dynabeads, Dynal Biotech) according to the manufacturer's instructions. This positive-selection process yielded over 98% $CD4^+$ T cells.

Fresh $CD4^+$ T cells and Mo-DCs isolated from the same healthy volunteer were used throughout this study.

[2] *Abbreviations used:* DC, dendritic cell; Mo-DC, monocyte-derived dendritic cell; PDTC, pyrrolidine dithiocarbamate; MVB, multivesicular body; CB, cacodylate buffer; MW, molecular weight; FSC, forward scatter; SSC, side scatter.

2.3. Exosome isolation and purification

Mo-DCs were generated from PBMCs with GM-CSF and IL-4 as described above. Seven days after the initiation of culture, Mo-DC culture supernatants were collected. Exosomes were isolated as previously described but with minor modifications [11,12]. Culture supernatants were centrifuged at 300*g* for 5 min and then at 1200*g* for 20 min to eliminate cells and debris. Cell-free supernatants were clarified through a 0.2-μm filter (Sartorius AG, Goettingen, Germany) to reduce the number of contaminating large vesicles shed from the plasma membrane. The clarified supernatant was subsequently concentrated through a 100-kDa membrane (YM-100, Microcon, Millipore, Billerica, MA, USA). In some experiments, this concentration procedure was repeated five times with PBS (Wako Pure Chemical Industries, Osaka, Japan) to eliminate the original culture supernatant. The concentrated materials were resuspended in RPMI medium at the original volume of the supernatant. This preparation was denoted crude exosomes.

Exosomes were further purified with human anti-HLA-DP, -DQ, or -DR-coated paramagnetic beads (average size: 4.5 μm, Dynal). Briefly, human anti-HLA-DP, -DQ, or -DR-coated paramagnetic beads were washed with PBS. And 1.0×10^6 DC-derived exosomes were mixed with 1.0×10^6 paramagnetic beads. The mixture was incubated at 4 °C for 24 h on a rotating plate, and the beads were washed twice on a magnetic rack with PBS containing 3% BSA (Sigma) and 0.1% NaN_3 (Sigma) (referred to as FACS buffer) to eliminate unbound or excess exosomes. Finally, exosomes coupled to the beads were resuspended in RPMI medium at the original volume of the exosome-containing medium. This preparation was denoted purified exosomes.

2.4. Naive $CD4^+$ T cell culture

$CD4^+$ T cells were suspended at a cell density of 1.0×10^6/ml, and 1.5×10^5 $CD4^+$ T cells were plated in a 96-well flat-bottomed culture plate (150 μl) and cultured at 37 °C for the indicated times. In an experiment using separated cell-culture system, $CD4^+$ T cells (1.5×10^6 cells) were cultured with Mo-DCs (1.5×10^5 cells) in 1.5 ml of RPMI medium or were cultured separately in RPMI medium (1.5 ml) with a 0.4-μm separated cell-culture system (Becton–Dickinson). Cellular viability and the number of $CD4^+$ T cells were determined by trypan blue dye exclusion and a cell counter (CDA-500, Sysmex Mundelin, IL, USA), respectively. T cells and DCs were easily distinguishable with each cell size using a cell counter.

2.5. Blocking assay for MHC class II molecules

To examine the effect of MHC class II proteins on Mo-DCs or of exosome preparations on naive $CD4^+$ T cell survival, Mo-DCs (1.0×10^5 cells/ml), crude exosomes, or purified exosomes prepared from 1×10^5 Mo-DC/ml were preincubated with anti-MHC class II mAb (4 μg/ml, Diaclone Research Besaucon, France) at 37 °C for 1 h, and $CD4^+$ T cells (1.0×10^6 cells/ml) were added and cultured at 37 °C for 4 days. Isotype-matched IgG1 mAb was used as a control.

2.6. FACS analysis

A 10× concentrate of crude exosomes (100 μl) was mixed with 100 μl FITC-conjugated anti-HLA-DR mAb and PE-conjugated anti-CD86 mAb. After a 30-min incubation at 4 °C, the samples were diluted with FACS buffer, and the fluorescence intensities of the exosome preparations were measured with a FACS Calibur flow cytometer and were analyzed with CELLQuest software.

Purified exosomes were prepared with human anti-HLA-DP, -DQ, or -DR-coated paramagnetic beads as described above. Purified exosomes (10 μl) were suspended in 100 μl FACS buffer, mixed with FITC-conjugated anti-HLA-DR mAb (10 μl) and PE-conjugated anti-CD86 mAb (10 μl), and incubated at 4 °C for 30 min. The samples were washed twice on a magnetic rack with FACS buffer, followed by reconstitution of the bead pellets in buffer containing 1% formaldehyde. Stained and fixed exosome-coupled beads were analyzed on a FACS Calibur flow cytometer with CELLQuest software.

2.7. Electrophoretic mobility shift assay

NF-κB activity in nuclei isolated from naive $CD4^+$ T cells was determined by electrophoretic mobility shift assay (EMSA). Extraction of nuclear proteins and EMSA were performed as described previously [27]. Briefly, 5 μg of nuclear protein was incubated for 30 min at room temperature with binding buffer (20 mM Hepes–NaOH, pH 7.9, 2 mM EDTA, 100 mM NaCl, 10% glycerol, and 0.2% NP-40), poly(dI–dC), and ^{32}P-labeled double-stranded oligonucleotide containing the NF-κB binding motif (Promega, Madison, WI, USA). The sequence of the double-stranded oligomer used for EMSA is as follows: 5′-AGTTGAGGGGACTTTCCC AGGC-3′ (sense strand). The reaction mixtures were loaded on a 4% polyacrylamide gel and electrophoresed with running buffer 0.25× TBE. After the gel was dried, DNA–protein complexes were visualized by autoradiography.

2.8. Electron microscopy

Exosome-bead complexes were fixed in 3% glutaraldehyde in 0.1 M cacodylate buffer (CB) at pH 7.3 for 3 h at 4 °C and washed in 0.1 M CB. The complexes were resuspended and embedded in 4% agar [28]. After the

agar was cut into 1-mm^3 pieces, the pieces were fixed in 1% osmium tetroxide in 0.1 M CB overnight and washed in distilled water. The specimens were dehydrated in a graded series of ethanol and embedded in Epon 812. Ultrathin sections were treated with uranyl acetate followed by lead citrate and were examined with an electron microscope (JEM-1200EX, JEOL, Tokyo, Japan).

2.9. Statistical analysis

Comparison of means among three or more groups was done by the Scheffé's method. All results with a p value of less than 0.05 were considered statistically significant.

3. Results

3.1. Mo-DCs support naive CD4$^+$ T cell survival

When naive CD4$^+$ T cells were cultured in RPMI medium in the absence of Mo-DCs, CD4$^+$ T cell numbers decreased daily. Coculture of CD4$^+$ T cells with Mo-DCs at a ratio of 10:1 significantly supported CD4$^+$ T cell survival (Fig. 1A). Mo-DCs supported CD4$^+$ T cell survival in a dose-dependent manner (Fig. 1B). Taken together, CD4$^+$ T cells and Mo-DCs were principally used at a cell ratio of 10:1 throughout this study. To examine whether direct contact between CD4$^+$ T cells and Mo-DCs was required to support CD4$^+$ T cell survival, we used a separated cell-culture system as described in Materials and methods. When CD4$^+$ T cells were cultured without direct contact with Mo-DCs, the number of CD4$^+$ T cells decreased compared to that in mixed cultures but increased significantly compared to that of CD4$^+$ T cells alone (Fig. 2A). Because it is believed that small Mo-DC-derived components that can pass through 0.4-μm filters may have a supportive effect on naive CD4$^+$ T cell survival, we speculated that cytokines such as IL-4, IL-7, or IL-15 may be involved. Culture supernatants were filtered with a filter that allows components smaller than 100 kDa to pass through. Both passed (cytokine-rich) and nonpassed (cytokine-poor) fractions were re-adjusted to the original volume with RPMI medium. Contrary to our expectation, the nonpassed fraction but not the passed fraction supported naive CD4$^+$ T cell survival (Fig. 2B).

We next examined which molecules contribute to the prolonged in vitro survival of naive CD4$^+$ T cells. We focused on MHC class II proteins, particularly HLA-DR, which is expressed on Mo-DCs. Pretreatment of Mo-DCs with anti-HLA-DR mAb inhibited the supportive effect on CD4$^+$ T cell survival (Fig. 3A). Interestingly, addition of anti-HLA-DR mAb to the nonpassed fraction also significantly decreased the number of cells (Fig. 3B).

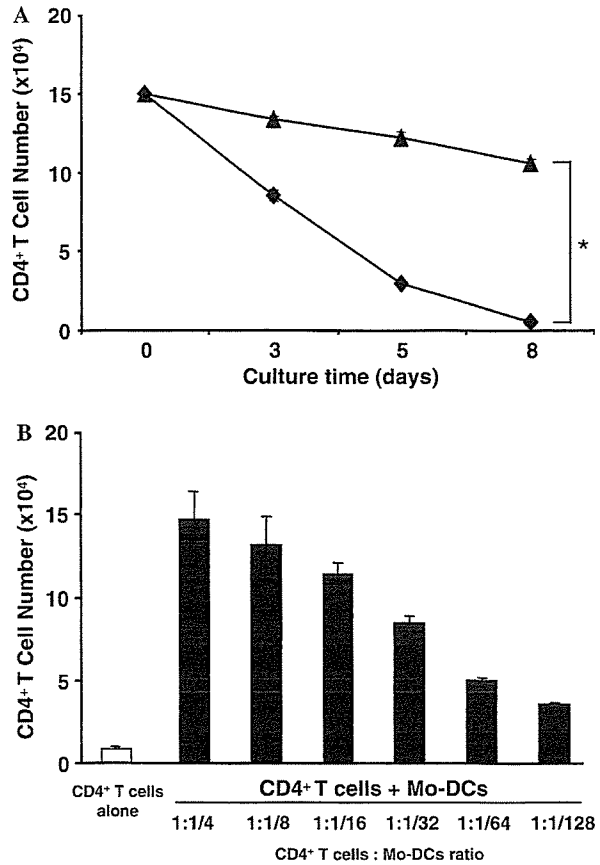

Fig. 1. Coculture with Mo-DCs supports naive CD4$^+$ T cell survival. (A) Purified naive CD4$^+$ T cells were cultured in RPMI medium with (closed triangle) or without (closed diamond) autologous Mo-DCs at a ratio of 10:1. Cell numbers of the viable CD4$^+$ T cells were counted on the indicated days after dead cell exclusion by trypan blue staining. Values represent the means ± SD of triplicate determinations. The asterisk indicates significant differences <0.0001. The data are representative of six independent experiments using Mo-DCs and CD4$^+$ T cells obtained from three different healthy donors. (B) Mo-DCs support naive CD4$^+$ T cell survival in a dose-dependent manner. Purified naive CD4$^+$ T cells (1.5×10^5/150 μl) were cultured with indicated cell numbers of Mo-DCs for 5 days. The data are representative of three independent experiments using Mo-DCs and CD4$^+$ T cells obtained from three different healthy donors.

3.2. Exosomes are present in Mo-DC culture supernatant

We speculated that the HLA-DR-bearing components in the nonpassed fraction may be insoluble substances such as membrane fragments or exosomes. Crude exosomes and purified exosomes were collected from Mo-DC culture supernatants as described in Materials and methods. FACS analysis revealed that 21.5% of the particles in the crude exosomes were positive for both HLA-DR and CD86 (data not shown). The FACS cytogram of purified exosomes coupled to mAb-coated beads showed three populations: single beads, clumps of two beads, and clumps of three or more beads, from the dot-plot representation of forward and side scatter (Fig. 4A-1), as described previously [29]. Single beads represented more

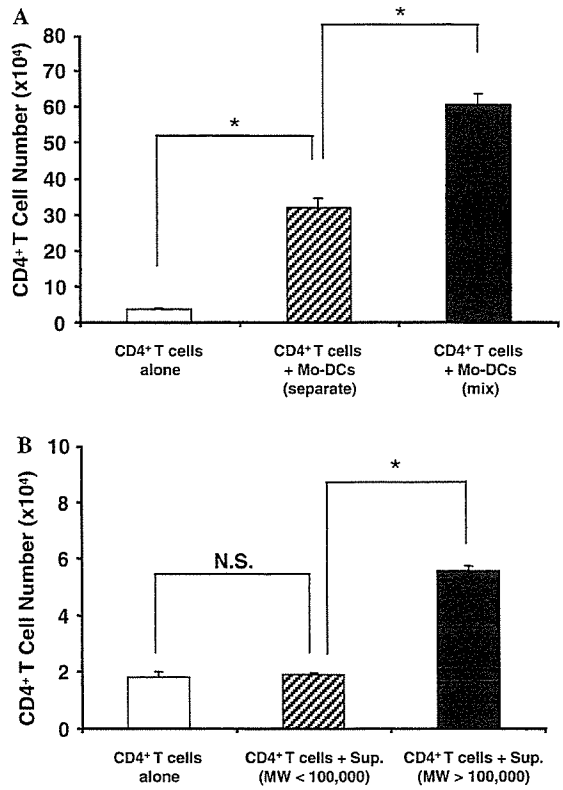

Fig. 2. Supportive effects of Mo-DCs on naive $CD4^+$ T cell survival without direct cellular contact. (A) Viable cell numbers of naive $CD4^+$ T cells cultured in chambers separated by a membrane with pores from Mo-DCs (hatched column) or in the mixture without separation (filled column) were counted on day 5. In only this experiment using separated cell-culture system, $CD4^+$ T cells (1.5×10^6 cells) were cultured with Mo-DCs (1.5×10^5 cells) in 1.5 ml of RPMI medium or were cultured separately in RPMI medium (1.5 ml) with a 0.4-μm separated cell-culture system. Open column shows the cell number of viable naive $CD4^+$ T cells cultured without Mo-DCs. Values represent means ± SD of triplicate determinations. The asterisks indicate significant differences <0.0001. The data are representative of three independent experiments using Mo-DCs and $CD4^+$ T cells obtained from three different healthy donors. (B) Naive $CD4^+$ T cells were cultured in the presence of the culture supernatant of Mo-DCs for 3 days and then the viable cell numbers of the cells were counted. Each column shows the viable cell numbers of the T cells cultured with components smaller than MW 100,000 (hatched column), those larger than MW 100,000 (closed column) or RPMI medium only (open column). Values represent means ± SD of triplicate determinations. The asterisk indicates significant differences 0.0004. N.S. shows not significant. The data are representative of three independent experiments using Mo-DCs and $CD4^+$ T cells obtained from three different healthy donors.

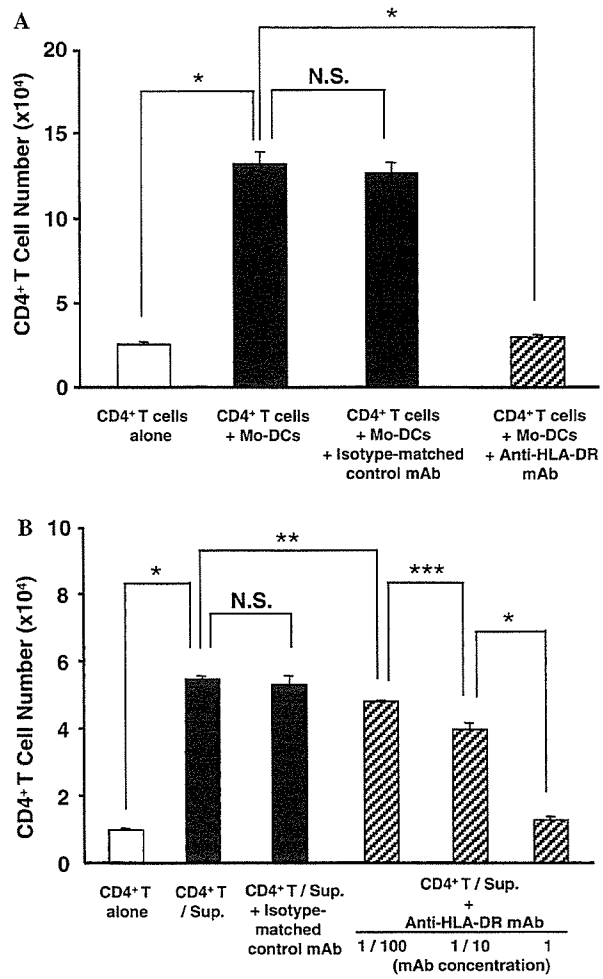

Fig. 3. Requirement of TCR-MHC class II interaction for the prolonged naive $CD4^+$ T cells survival. (A) Viable cell numbers of naive $CD4^+$ T cells cultured with Mo-DCs for 5 days in the presence of anti-MHC class II mAb (4 μg/ml) (hatched column) or isotype-matched control mAb (closed column) were shown. The asterisk indicates significant differences <0.0001. N.S. shows not significant. (B) Naive $CD4^+$ T cells were cultured in the presence of the culture supernatant of Mo-DCs (components of larger than MW 100,000) with anti-MHC class II mAb (hatched column) or with isotype-matched control mAb (closed column) for 4 days and then the viable cell numbers of the cells were counted. The asterisks indicate significant differences <0.0001 (*), 0.002 (**), and 0.007 (***). N.S. shows not significant. Values represent means ± SD of triplicate determinations. The data are representative of three independent experiments using Mo-DCs and $CD4^+$ T cells obtained from three different healthy donors.

than 85% of the total number. The populations containing clumped beads were removed from the analysis by gating for single beads only. More than 90% of the single beads were positive for both HLA-DR and CD86 (Fig. 4A-2). These data indicate that 20% of the particles in the crude exosomes and 90% of the particles in the purified exosomes consist of intact HLA-DR- and CD86-expressing exosomes. Electron microscopic analysis confirmed that the substances coupled to the beads were exosomes (Figs. 4B-1 and B-2). These substances showed the characteristic saucer-like morphology of a flattened sphere limited by a lipid bilayer. The exosomes coupled to the beads ranged from 40 to 140 nm in diameter (means ± SD, 78.46 ± 11.04 nm). The average size of a bead and a $CD4^+$ T cell is 4500 and 7250 nm, respectively.

3.3. Mo-DC-derived exosomes support naive $CD4^+$ T cell survival

To confirm that exosomes are involved in supporting in vitro naive $CD4^+$ T cell survival, purified exosomes

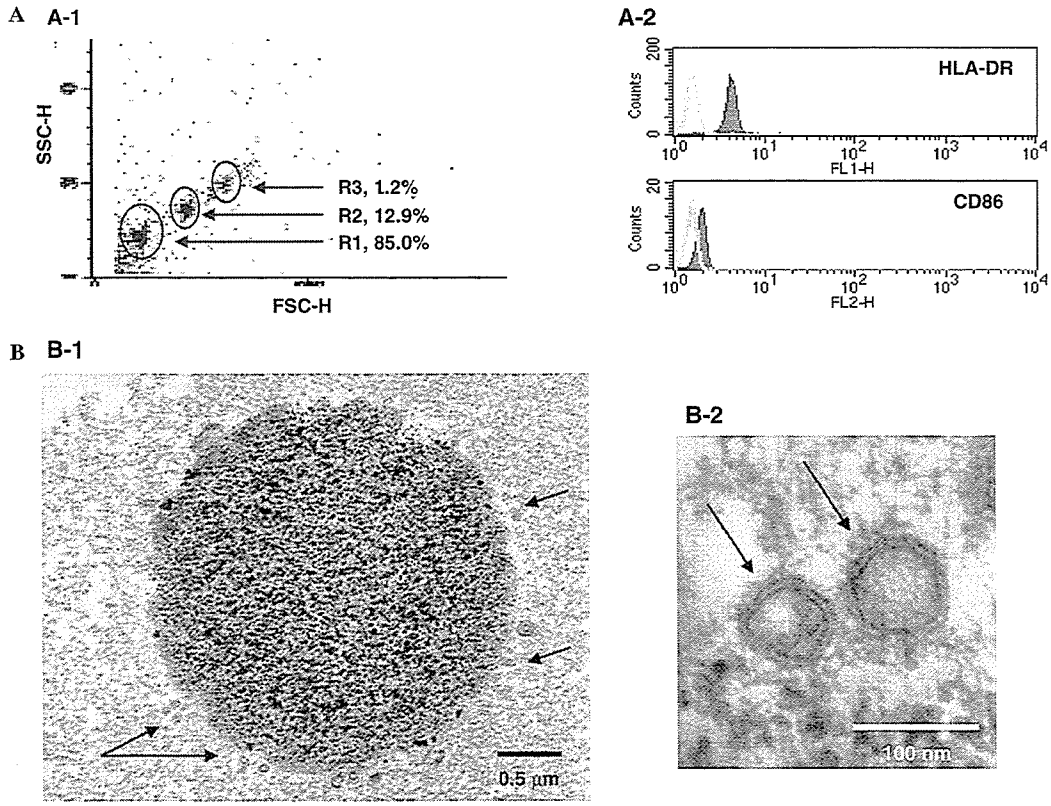

Fig. 4. Detection of MHC class II and CD86 molecules in the components of over MW 100,000 supernatant and electron microscopic characterization of the component. (A) Purified components in supernatants coupled with anti-HLA-DR mAb-coated beads were stained with anti-HLA-DR or anti-CD86 mAbs, and then analyzed by FACS. Three populations of the stained beads appeared in the forward (FSC) and side scatter (SSC) plot are indicated as R1, R2, and R3, respectively and the percentages of each population are also shown (A-1). Histograms show staining of beads for anti-HLA-DR or anti-CD86 (filled line) or control IgG (bold line) on gated R1 area (A-2). The data are representative of three independent experiments. (B) Purified components in supernatants coupled with beads were characterized by electron microscope. Small vesicles (arrows) coating on the surface of the bead (B-1), bar = 0.5 μm and two vesicles of higher magnification (B-2) are shown, bar = 100 nm. The data are representative of six independent experiments using Mo-DCs and $CD4^+$ T cells obtained from three different healthy donors.

coupled to mAb-coated beads were used as effector components. Purified exosomes but not beads alone significantly supported naive $CD4^+$ T cell survival in a dose-dependent manner (Fig. 5A). When beads alone were added to $CD4^+$ T cells, several dying cells were found, and the beads did not bind firmly to any $CD4^+$ T cells. When exosome-coupled beads (purified exosomes) were added to $CD4^+$ T cells, only a few dying cells were found, and the beads bound firmly to several living $CD4^+$ T cells (Fig. 5B). Anti-HLA-DR mAb abrogated the supportive effect of purified exosomes on naive $CD4^+$ T cell survival (Fig. 5C). Anti-HLA-DR mAb also inhibited the binding of exosome-coupled beads to naive $CD4^+$ T cells (data not shown).

3.4. Exosomes induce NF-κB activation in naive $CD4^+$ T cells

We hypothesized that interaction between HLA-DR on exosomes and TCRs on $CD4^+$ T cells induces NF-κB activation, and, as a result, these cells can survive even in severe culture conditions. NF-κB activation of naive $CD4^+$ T cells was estimated by EMSA. Crude exosomes induced NF-κB activation in naive $CD4^+$ T cells within 30 min. Specificity of DNA binding was confirmed by a competition study with a 50-fold excess of unlabeled oligonucleotide. Anti-HLA-DR mAb (4 μg/ml) was added to crude exosomes 1 h prior to coculture with naive $CD4^+$ T cells. Treatment with anti-HLA-DR mAb suppressed exosome-induced NF-κB activation. A NF-κB inhibitor, PDTC (100 μM), was added to naive $CD4^+$ T cells 1 h prior to treatment with crude exosomes. PDTC inhibited nuclear translocation of NF-κB p65 (Fig. 6). PDTC inhibited the supportive effect of crude exosomes on naive $CD4^+$ T cell survival in a dose-dependent manner between 3 and 5 μM without significant direct cytotoxic effect (Fig. 7). These data suggest that exosome-induced NF-κB activation plays a critical role in the survival of naive $CD4^+$ T cells in vitro.

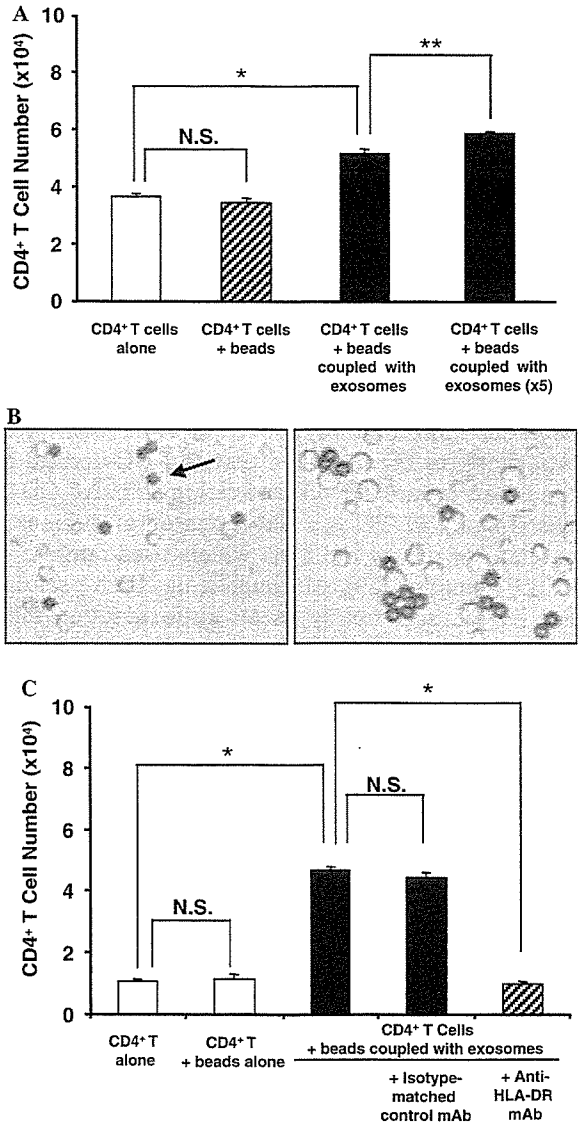

Fig. 5. Prolonged survival of naive $CD4^+$ T cells by interaction with exosomes coupled to anti-MHC class II mAb-coated beads. (A) Viable cell numbers of naive $CD4^+$ T cells cultured with exosomes coupled to anti-MHC class II mAb-coated beads (closed column) for 5 days are shown. Viable cell numbers of $CD4^+$ T cells alone (open column) and $CD4^+$ T cells with anti-HLA-DR mAb-coated beads only (hatched column) are also shown. The asterisk indicates significant differences <0.0001 (*) and 0.0029 (**). N.S. shows not significant. The data are representative of three independent experiments using Mo-DCs and $CD4^+$ T cells obtained from three different healthy donors. (B) Phase-contrast photomicrographs of $CD4^+$ T cells 5 days after coculture with beads (arrow) alone (left panel) and beads coupled with exosomes (right panel). The pictures are representative of three independent experiments using Mo-DCs and $CD4^+$ T cells obtained from three different healthy donors. (C) Viable cell numbers of $CD4^+$ T cells cultured with exosome-coupled beads in the presence (hatched column) or the absence (closed column) of anti-HLA-DR mAb or in the presence (closed column) of isotype-matched control mAb. Open column shows the viable cell number of $CD4^+$ T cells alone and $CD4^+$ T cells cultured with beads alone. The asterisk indicates significant differences <0.0001. N.S. shows not significant. Values represent means ± SD of triplicate determinations. The data are representative of three independent experiments using Mo-DCs and $CD4^+$ T cells obtained from three different healthy donors.

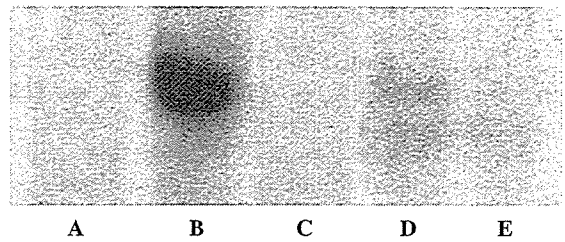

Fig. 6. NF-κB activation in naive $CD4^+$ T cells induced by crude exosomes. The nuclear translocation of NF-κB p65 of naive $CD4^+$ T cells in response to exosomes was determined by EMSA. Naive $CD4^+$ T cells were incubated for 30 min for various conditions as below. Lane A, medium only; lane B, crude exosomes; lane C, crude exosomes with NF-κB ODN (50×); lane D, crude exosomes with anti-HLA-DR mAb; and lane E, crude exosomes with PDTC (100 μM). The data are representative of three independent experiments using Mo-DCs and $CD4^+$ T cells obtained from three different healthy donors.

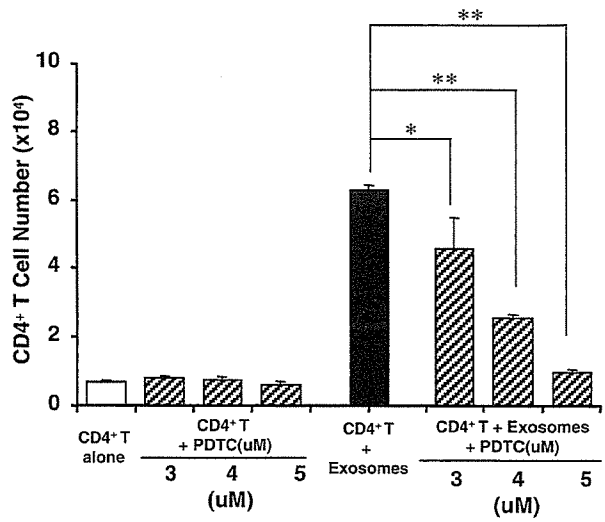

Fig. 7. Suppression of exosome-induced prolonged survival of naive $CD4^+$ T cells by NF-κB inhibitor PDTC. Viable cell numbers of naive $CD4^+$ T cells cultured with crude exosomes (closed column), crude exosomes with indicated concentrations of PDTC (hatched column) or medium alone (open column) for 5 days are shown. The asterisks indicate significant differences 0.0016 (*), <0.0001 (**). Values represent means ± SD of triplicate determinations. The data are representative of three independent experiments using Mo-DCs and $CD4^+$ T cells obtained from three different healthy donors.

4. Discussion

We showed that Mo-DC-derived exosomes can prolong naive $CD4^+$ T cell survival in an HLA-DR-dependent manner. Our data also suggest that NF-κB activation induced by exosomes contributes to this increased survival.

Several players such as TCRs and CD28 are related to T cell survival [5,30]. In the last two decades, many in vivo studies in mice have shown that long-term survival of naive $CD4^+$ T cells requires interaction with self-MHC class II proteins [1–3]. However, it remains

unclear whether interaction with these proteins can prolong the short-term survival of naive $CD4^+$ T cells in vitro. Recently, it was shown that human Mo-DCs expressing abundant MHC class II proteins are able to support short-term survival of T cells in vitro [7]. Interestingly, our present findings indicate that although HLA-DR is critical for naive $CD4^+$ T cell survival in vitro (Fig. 3A), direct interaction between Mo-DCs and T cells is not always required (Fig. 2A). It has been shown that MHC class II proteins are very abundant in exosomes from APCs [10]. In the present study, Mo-DCs also released exosomes into culture medium, and Mo-DC-derived exosomes expressed both MHC class II and CD86 proteins (Fig. 4A). Recently, it was reported that MHC class II proteins on released exosomes are functional [10,31]. Raposo et al. [10] showed that exosomes derived from both human and murine B lymphocytes induce antigen-specific MHC class II-restricted T cell responses. Vincent-Schneider et al. [31] showed that the combination of exosomes with DCs results in highly efficient stimulation of specific T cells and suggested that exosome-bearing MHC class II complexes are taken up by dedicated APCs for efficient T cell activation. On the basis of these findings, we hypothesized that Mo-DC-derived exosomes can prolong naive $CD4^+$ T cell survival. To prove this, we used exosomes purified with human anti-HLA-DP, -DQ, or -DR-coated paramagnetic beads. To avoid contamination with serum-derived exosomes [32], we used RPMI 1640 medium supplemented with 1% human albumin. Purified exosomes prolonged naive $CD4^+$ T cell survival in an HLA-DR-dependent manner (Fig. 5C).

The present study shows a novel function of exosomes. Mo-DC-derived exosomes express not only MHC class II but also CD86 proteins. CD28, which is a ligand for CD86, is believed to contribute to T cell survival [29]. In our study, peripheral monocytes, in which CD86 expression is weak, did not prolong $CD4^+$ T cell survival (data not shown), suggesting a possible role of a CD28/CD86 interaction. But our data that specific antibody against HLA-DR inhibited completely the effect of exosomes on $CD4^+$ T cell survival. These data indicate that TCR is a likely candidate for transmitting the viability signal. However, participation of other receptors for MHC class II such as LAG-3 has not been excluded [33]. Furthermore, other molecular events, such as CD28/CD86 interaction, in addition to the interaction between TCR and HLA-DR may operate in prolongation of $CD4^+$ T cell survival induced with exosomes. A role of exosome-bearing CD86 in $CD4^+$ T cell survival has not been reported, and the mechanism of exosome-induced, HLA-DR-dependent naive $CD4^+$ T cell survival is not clear. Several transcription factors such as Ets, NFAT, AP-1, and NF-κB have been shown to be activated by TCRs or CD28 [20]. Recent studies have indicated that NF-κB plays a key role in T cell survival. For example, it has been suggested that the PI3K/Akt pathway is important for the effects of both CD28 and IL-2R [23,34,35], and NF-κB is thought to be target of Akt [36,37]. More direct evidence that NF-κB contributes to T cell survival has been reported recently [22,26]. In p50−/− cRel−/− mice, which exhibit virtually no inducible κB site binding activity, an essential role of TCR-induced NF-κB was indicated in T cell survival [26]. In addition, NF-κB regulated TCR-induced expression of anti-apoptotic Bcl-2 family members and NF-κB activation was not only necessary but was also sufficient for T cell survival [38]. Wan and DeGregon [22] reported that the survival of antigen-stimulated T cells requires NF-κB-mediated inhibition of p73 expression. Our present data show for the first time that Mo-DC-derived exosomes can induce NF-κB activation in naive $CD4^+$ T cells (Fig. 6). PDTC is a stable analog of dithiocarbamate and is one of the most widely used inhibitors of NF-κB signaling [39]. Although it has been postulated that PDTC acts simply as an antioxidant to inhibit NF-κB activation [40], it has been shown definitively that PDTC inhibits NF-κB activation independently of antioxidative function [41]. In the present study, we used PDTC to examine contribution of the NF-κB pathway to exosome-mediated $CD4^+$ T cell survival. PDTC inhibited the supportive effect of exosomes on $CD4^+$ T cell survival in a dose-dependent manner without significant direct cytotoxic effect (Fig. 7). These results suggest that NF-κB plays an essential role in exosome-mediated $CD4^+$ T cell survival. However, we have no definitive evidence as to how exosomes induce NF-κB in naive $CD4^+$ T cells.

It has been reported that DC-derived exosomes may be used as vectors for vaccination because they express high levels of functional MHC class I– and class II–peptide complexes, together with CD86 [10,14,19]. A recent report showed that MHC class I proteins on purified exosomes from DCs can be directly loaded with peptide at much greater levels than by indirect loading [17]. Also reported was a new exosome purification procedure from Mo-DCs [14], in which ultrafiltration through a 500-kDa membrane and ultracentrifugation into a 30% sucrose/deuterium-oxide cushion made it possible to recover up to 50% exosomes. Although the function of most of the exosome-bearing proteins is unknown at present, accumulated data on exosome function suggest that these proteins will become exciting therapeutic tools in the near future.

Acknowledgments

We thank Yasuhiro Hirakawa (Department of Anatomy and Cell Biology affiliation), Takaaki Kanemaru, and Kaori Nomiyama for technical assistance.

References

[1] S. Takeda, H.R. Rodewald, H. Arakawa, H. Bluethmann, T. Shimizu, MHC class II molecules are not required for survival of newly generated CD4$^+$ T cells, but affect their long-term life span, Immunity 5 (1996) 217–228.

[2] T. Brocker, Survival of mature CD4 T lymphocytes is dependent on major histocompatibility complex class II-expressing dendritic cells, J. Exp. Med. 186 (1997) 1223–1232.

[3] S. Garcia, J. DiSanto, B. Stockinger, Following the development of a CD4 T cell response in vivo: from activation to memory formation, Immunity 1 (1999) 163–171.

[4] C. Tanchot, F.A. Lemonnier, B. Perarnau, A.A. Freitas, B. Rocha, Differential requirements for survival and proliferation of CD8 naive or memory T cells, Science 276 (1997) 2057–2062.

[5] J. Kirberg, A. Berns, H. von Boehmer, Peripheral T cell survival requires continual ligation of the T cell receptor to major histocompatibility complex-encoded molecules, J. Exp. Med. 186 (1997) 1269–1275.

[6] C. Viret, F.S. Wong, C.A. Janeway Jr., Designing and maintaining the mature TCR repertoire: the continuum of self-peptide:self-MHC complex recognition, Immunity 10 (1999) 559–568.

[7] T. Kondo, I. Cortese, S. Markovic-Plese, K.P. Wandinger, C. Carter, M. Brown, S. Leitman, R. Martin, Dendritic cells signal T cells in the absence of exogenous antigen, Nat. Immunol. 2 (2001) 932–938.

[8] E.G. Trams, C.J. Lauter, N. Salem Jr., U. Heine, Exfoliation of membrane ecto-enzymes in the form of micro-vesicles, Biochim. Biophys. Acta 645 (1981) 63–70.

[9] R.M. Johnstone, M. Adam, J.R. Hammond, L. Orr, C. Turbide, Vesicle formation during reticulocyte maturation. Association of plasma membrane activities with released vesicles (exosomes), J. Biol. Chem. 262 (1987) 9412–9420.

[10] G. Raposo, H.W. Nijman, W. Stoorvogel, R. Liejendekker, C.V. Harding, C.J. Melief, H.J. Geuze, B lymphocytes secrete antigen-presenting vesicles, J. Exp. Med. 183 (1996) 1161–1172.

[11] J.Q. Davis, D. Dansereau, R.M. Johnstone, V. Bennett, Selective externalization of an ATP-binding protein structurally related to the clathrin-uncoating ATPase/heat shock protein in vesicles containing terminal transferrin receptors during reticulocyte maturation, J. Biol. Chem. 261 (1986) 15368–15371.

[12] C. Thery, M. Boussac, P. Veron, P. Ricciardi-Castagnoli, G. Raposo, J. Garin, S. Amigorena, Proteomic analysis of dendritic cell-derived exosomes: a secreted subcellular compartment distinct from apoptotic vesicles, J. Immunol. 166 (2001) 7309–7318.

[13] F. Sallusto, A. Lanzavecchia, Efficient presentation of soluble antigen by cultured human dendritic cells is maintained by granulocyte/macrophage colony-stimulating factor plus interleukin 4 and downregulated by tumor necrosis factor alpha, J. Exp. Med. 179 (1994) 1109–1118.

[14] L. Zitvogel, A. Regnault, A. Lozier, J. Wolfers, C. Flament, D. Tenza, P. Ricciardi-Castagnoli, G. Raposo, S. Amigorena, Eradication of established murine tumors using a novel cell-free vaccine: dendritic cell-derived exosomes, Nat. Med. 4 (1998) 594–600.

[15] H.G. Lamparski, A. Metha-Damani, J.Y. Yao, S. Patel, D.H. Hsu, C. Ruegg, J.B. Le Pecq, Production and characterization of clinical grade exosomes derived from dendritic cells, J. Immunol. Methods 270 (2002) 211–226.

[16] C. Thery, L. Duban, E. Segura, P. Veron, O. Lantz, S. Amigorena, Indirect activation of naive CD4$^+$ T cells by dendritic cell-derived exosomes, Nat. Immunol. 3 (2002) 1156–1162.

[17] D.H. Hsu, P. Paz, G. Villaflor, A. Rivas, A. Mehta-Damani, E. Angevin, L. Zitvogel, J.B. Le Pecq, Exosomes as a tumor vaccine: enhancing potency through direct loading of antigenic peptides, J. Immunother. 26 (2003) 440–450.

[18] I. Hwang, X. Shen, J. Sprent, Direct stimulation of naive T cells by membrane vesicles from antigen-presenting cells: distinct roles for CD54 and B7 molecules, Proc. Natl. Acad. Sci. USA 100 (2003) 6670–6675.

[19] D. Skokos, H.G. Botros, C. Demeure, J. Morin, R. Peronet, G. Birkenmeier, S. Boudaly, S. Mecheri, Mast cell-derived exosomes induce phenotypic and functional maturation of dendritic cells and elicit specific immune responses in vivo, J. Immunol. 170 (2003) 3037–3045.

[20] C.T. Kou, J.M. Leiden, Transcriptional regulation of T lymphocyte development and function, Annu. Rev. Immunol. 17 (1999) 149–187.

[21] E. Dudley, F. Hornung, L. Zheng, D. Scherer, D. Ballard, M. Lenardo, NF-kappaB regulates Fas/APO-1/CD95- and TCR-mediated apoptosis of T lymphocytes, Eur. J. Immunol. 29 (1999) 878–886.

[22] Y.Y. Wan, J. DeGregon, The survival of antigen-stimulated T cells requires NFkappaB-mediated inhibition of p73 expression, Immunity 18 (2003) 331–342.

[23] R.G. Jones, M. Parsons, M. Bonnard, V.S. Chan, W.C. Yeh, J.R. Woodgett, P.S. Ohashi, Protein kinase B regulates T lymphocyte survival, nuclear factor kappaB activation, and Bcl-X(L) levels in vivo, J. Exp. Med. 191 (2000) 1721–1734.

[24] S. Ghosh, M.J. May, E.B. Kopp, NF-kB and Rel proteins: evolutionarily conserved mediators of immune responses, Annu. Rev. Immunol. 16 (1998) 225–260.

[25] J.A. DiDonato, F. Mercurio, M. Karin, Phosphorylation of IkB precedes but is not sufficient for its dissociation from NF-kB, Mol. Cell. Biol. 15 (1995) 1302–1311.

[26] Y. Zheng, M. Vig, J. Lyons, L. Van Parijs, A.A. Bed, Combined deficiency of p50 and cRel in CD4$^+$ T cells reveals an essential requirement for nuclear factor kappa B in regulating mature T cell survival and in vivo function, J. Exp. Med. 197 (2003) 861–874.

[27] M. Kojima, T. Morisaki, K. Izuhara, A. Uchiyama, Y. Matsunari, M. Katano, M. Tanaka, Lipopolysaccharide increase cyclooxygenase-2 expression in a colon carcinoma cell line through nuclear factor-kappa B activation, Oncogene 19 (2000) 1225–1231.

[28] J.A. Hobot, E. Carlemalm, W. Villiger, E. Kellenberger, Periplasmic gel: new concept resulting from the reinvestigation of bacterial cell envelope ultrastructure by new methods, J. Bacteriol. 160 (1984) 143–152.

[29] A. Clayton, J. Court, H. Navabi, M. Adams, M.D. Mason, J.A. Hobot, G.R. Newman, B. Jasani, Analysis of antigen presenting cell derived exosomes, based on immuno-magnetic isolation and flow cytometry, J. Immunol. Methods 247 (2001) 163–174.

[30] L.H. Boise, A.J. Minn, P.J. Noel, C.H. June, M.A. Accavitti, T. Lindsten, C.B. Thompson, CD28 costimulation can promote T cell survival by enhancing the expression of Bcl-XL, Immunity 3 (1995) 87–98.

[31] H. Vincent-Schneider, P. Stumptner-Cuvelette, D. Lankar, S. Pain, G. Raposo, P. Benaroch, C. Bonnerot, Exosomes bearing HLA-DR1 molecules need dendritic cells to efficiently stimulate specific T cells, Int. Immunol. 14 (2002) 713–722.

[32] G. van Niel, G. Raposo, C. Candalh, M. Boussac, R. Hershberg, N. Cerf-Bensussan, M. Heyman, Intestinal epithelial cells secrete exosome-like vesicles, Gastroenterology 121 (2001) 337–349.

[33] C.J. Workman, D.A. Vignali, The CD4-related molecule, LAG-3 (CD223), regulates the expansion of activated T cells, Eur. J. Immunol. 33 (2003) 970–979.

[34] J.S. Burr, N.D. Savage, G.E. Messah, S.L. Kimzey, A.S. Shaw, R.H. Arch, J.M. Green, Cutting edge: distinct motifs within CD28 regulate T cell proliferation and induction of Bcl-XL, J. Immunol. 166 (2001) 5331–5335.

[35] K.A. Frauwirth, J.L. Riely, M.H. Harris, R.V. Parry, J.C. Rathmell, D.R. Plas, R.L. Elstrom, C.H. June, C.B. Thompson, The CD28 signaling pathway regulates glucose metabolism, Immunity 16 (2002) 769–777.

[36] L.P. Kane, V.S. Shapiro, D. Stokoe, A. Weiss, Induction of NF-kappaB by the Akt/PKB kinase, Curr. Biol. 9 (1999) 601–604.
[37] J.A. Romashkova, S.S. Makarov, NF-kappaB is a target of AKT in anti-apoptotic PDGF signaling, Nature 401 (1999) 86–90.
[38] R.J. Grumont, I.J. Rourke, S. Gerondakis, Rel-dependent induction of A1 transcription is required to protect B cells from antigen receptor ligation-induced apoptosis, Genes Dev. 13 (1999) 400–411.
[39] P.A. Baeuerle, T. Henkel, Function and activation of NF-kB in the immune system, Annu. Rev. Immunol. 12 (1994) 141–179.
[40] L. Flohe, R. Brigelius-Flohe, C. Saliou, M.G. Traber, L. Packer, Redox regulation of NF-kappa B activation, Free Radic. Biol. Med. 22 (1997) 1115–1126.
[41] M. Hayakawa, H. Miyashita, I. Sakamoto, M. Kitagawa, H. Tanaka, H. Yasuda, M. Karin, K. Kikugawa, Evidence that reactive oxygen species do not mediate NF-kB activation, EMBO J. 22 (2003) 3356–3366.

Parasitology Research
© Springer-Verlag 2005
DOI 10.1007/s00436-004-1296-0

Original Paper

Expression of TGF-β-like molecules in the life cycle of *Schistosoma japonicum*

M. Hirata (✉) · K. Hirata · T. Hara · M. Kawabuchi · T. Fukuma

M. Hirata · T. Hara · T. Fukuma
Department of Parasitology, Kurume University School of Medicine, 830-0011 Kurume, Japan

K. Hirata · M. Kawabuchi
Department of Anatomy and Cell Biology, Graduate School of Medical Sciences, Kyushu University, 812-8582 Fukuoka , Japan

✉ M. Hirata
Phone: +81-942-317550
Fax: +81-942-310344
E-mail: hiramizu@med.kurume-u.ac.jp

Received: 19 November 2004 / **Accepted:** 23 November 2004

Abstract The transforming growth factor β (TGF-β) family controls an extremely wide range of biological activities, such as the growth and differentiation of cells, and immunological events against infectious agents. Although TGF-β homologs appear to be widely present in metazoan animals, studies of parasite-derived molecules are relatively few. Using antibodies against anti-mouse TGF-β_1, -β_2, and -β_3, we show the expression of TGF-β-like molecules in *Schistosoma japonicum* cercariae, schistosomula, eggs and adult worms. Intense immunoreactivity was found on the surface of free-living cercarial bodies. In transverse sections of cercariae, the molecules were localized in the tegument and subtegumental cells, and the number and distribution of producing cells significantly differed with each antibody. In the skin-migrating stage, the expression in the tegumental surface gradually decreased and became almost negative within 48 h of exposure. In adult worms and eggs, the reactivity was found in subtegumental cells and in cells of a tubular structure, respectively. In western blot analysis, the detection of conventional TGF-β molecules failed. The expression of TGF-b-like molecules was distinctly regulated at each developmental stage.

Introduction

Transforming growth factor-β (TGF-β) is produced by a variety of mammalian host cells and plays a diversity of roles. The TGF-β family is essential for the growth and differentiation of cells and for morphogenesis (Kingsley 1994), and TGF-β is also an important modulator of immune cell activities, together with IL-4 and IL-10 (Letterio and Roberts 1998; Cobbold and Waldmann 1998). Induction and production of TGF-β during microbe infection has been reported to seriously affect the outcome of the disease (reviewed by Omer et al. 2000). In *Schistosoma mansoni* infection, TGF-β has been reported to be significantly involved in the regulation of macrophage cytotoxic activity (Oswald et al. 1992; Williams et al. 1995), or in the granulomatous response against eggs (Wahl et al. 1997; Mola et al. 1999).

The TGF-β family, related homologs and their corresponding receptors appear to be anciently conserved from nematodes to mammals. *Caenorhabditis elegans*, a well-studied free-living soil nematode, utilizes the TGF-β signaling system in dauer formation (Riddle and Albert 1997). The presence of two TGF-β homologs has been reported in parasitic nematodes: *tgh-1* in *Brugia malayi* and *B. pahangi* (Gomez-Escobar et al. 1998), and *tgh-2* in *B. malayi* (Gomez-Escobar et al. 2000). The type I TGF-β receptor, Bp-trk-1, has been isolated from the *Brugia* species (Gomez-Escobar et al. 1997). In *S. mansoni*, SmRK1, a member of TGF-β receptor family, is expressed on the surface of male worms (Davies et al. 1998; Beall et al. 2000) and host-derived TGF-β is a ligand of SmRK1 (Beall and Pearce 2001).

Schistosoma japonicum parasites are multicellular eukaryotic organisms that have a complex life cycle and are prevalent in South-east Asia. Schistosome worms settle in the portal vein and the eggs, which are continuously laid, cause severe intestinal and hepatosplenic disease. Here, we report that TGF-β immunoreactive molecules are expressed during the whole life cycle of *S. japonicum* (eggs, cercariae, schistosomula and adult worms), and that they are distinctly regulated at each developmental stage.